Defect and Diffusion Forum
ISSN: 1662-9507, Vol. 452, pp 65-71
doi:10.4028/p-zY1ER5
© 2026 The Author(s). Published by Trans Tech Publications Ltd, Switzerland.
Submitted: 2025-09-28
Revised: 2025-12-19
Accepted: 2026-02-28
Online: 2026-05-18

Characterization of Deep Levels Introduced by Energy Filtered Ion Implantation with DLTS and MCTS in 4H-SiC

Hitesh Jayaprakash[1,3,4,a*], Manuel Belanche[2,b], Constantin Csato[3,c], Florian Krippendorf[3,d], Ulrike Grossner[2,e], Michael Rueb[3,f]

[1]Ernst-Abbe-Hochschule Jena, Carl-Zeiß-Promenade 2, 07745 Jena, Germany

[2]Advanced Power Semiconductor Laboratory, ETH Zurich, Physikstrasse 3, 8092 Zurich, Switzerland

[3]mi2-factory GmbH, Hans-Knöll-Straße 6, 07745 Jena, Germany

[4]Friedrich Alexander Universität, Cauerstrasse 6, 91058 Erlangen, Germany

[a*]hitesh.jayaprakash@eah-jena.de [b]belanche@aps.ee.ethz.ch, [c]constantin.csato@mi2-factory.com, [d]florian.krippendorf@mi2-factory.com, [e]ulrike.grossner@ethz.ch, [f]michael.rueb@mi2-factory.com

Keywords: 4H-SiC, DLTS, MCTS, energy filtered ion implantation.

Abstract. The extensive study of point defects in 4H-SiC over the past two decades has led to a comprehensive understanding of their influence on device performance. Specifically, the dominant defects $Z_{1/2}$ and $EH_{6/7}$ have been well-quantified and are now formally assigned to specific states of the carbon vacancy. Building upon this foundational knowledge, our study investigates the defect landscape created by the novel process of Energy-Filtered Ion Implantation (EFII). Using DLTS and MCTS measurements conducted within the temperature range of 50−650 K, we analyzed the trap levels created by 19 MeV Nitrogen implantation in as-grown 4H-SiC epitaxial wafer. The majority carrier (electrons) trap with DLTS measurements reveal the presence of prominent peaks associated with carbon complexes, labeled as ON0a (E_c - 0.586 eV) and ON0b / $Z_{1/2}$ at (E_c - 0.681 eV), along with smaller peaks in the shallow region and a broader peak identified as $EH_{6/7}$ at (E_c - 1.53 eV) as the deepest peak. Notably, the close proximity of the ON0b peak to the well-known $Z_{1/2}$ peak poses a significant challenge, preventing the definitive assignment of a defect structure to the known carbon complexes. On the contrary, minority carrier (holes) trap detection with MCTS reveal B-center at (E_V+ 0.24 eV) and (E_V + 0.33 eV) and a negligible shallow peak at (E_V + 0.22 eV) assigned as X center. There was no indication of D-center formation in the EFII implanted samples.

Introduction

As an emerging power device technology, 4H-SiC has become a preferred material for high-power applications due to its robust physical properties. Although 4H-SiC is a widely used polytype, point defects are common in as-grown (CVD) material, with carbon vacancies typically observed and labeled as $Z_{1/2}$ and $EH_{6/7}$ [1]. These defects can also be generated by external processes such as ion implantation, which is a key step for creating carriers for current flow modulation. The presence of these point defects critically influences device performance, most notably through their direct impact on carrier lifetime [2]. Given that carrier lifetime dictates key device performance parameters like on-resistance (R_{on}) and switching speed in fabricated power devices such as diodes and MOS-FETs, addressing these defects would improve device performance. Carbon vacancies, in particular, are known to act as dominant recombination centers for electron-hole recombination [3]. Post ion im-plantation, a high-temperature annealing step, typically performed at 1700 °C to activate the dopants in an argon atmosphere, is effective at recovering the crystal lattice and removing most implantation-induced defects, a deeper understanding of the resulting defect structures is necessary, especially with the introduction of novel processing techniques.

This article is an open access article under the terms and conditions of the Creative Commons Attribution (CC BY) license
(https://creativecommons.org/licenses/by/4.0)

Energy Filtered Ion Implantation (EFII) is a new technology that offers precision drift zone doping [4], making it a key enabler for a simplified approach for SiC Super-Junction devices by simply masking the implanted regions. However, the specific types of point defects generated by this novel technology remain unexplored. Therefore, this study aims to investigate the point defects and trap levels generated by 19 MeV Nitrogen implantation with this technique. EFII offers an implantation depth of approximately 8.5 µm in 4H-SiC for the afore-mentioned Nitrogen ion energy. The implanted samples were subsequently annealed at 1700 °C with carbon capping layer. Deep-Level Transient Spectroscopy (DLTS) and Minority Carrier Transient Spectroscopy (MCTS) measurements were per-formed on standard Schottky diodes fabricated on the implanted SiC samples to identify the peaks that correspond to trap levels existing between valance and conduction bands.

Experimental Approach

The experimental approach involved the preparation and characterization of three 4H-SiC epitaxial wafers. A pristine wafer from Vendor A with a 10 µm as-grown epitaxial layer and a doping concentration of 5E15 cm^{-3} was used as a reference without additional processes before Schottky diode fabrication. Two additional wafers from Vendor B, which were unintentionally doped with nitrogen (<5E14 cm^{-3}) with 5 µm epitaxial layer thickness, were used for nitrogen ion implantation with EFII technology at an energy of 19 MeV. To implant different nitrogen concentrations, the wafers were divided into quadrants. The first wafer L was implanted with target concentrations of 1E14, 5E14 , and 1E15 cm^{-3} , while the second wafer G was implanted with 1E15 , 5E15 , and 1E16 cm^{-3} concentrations, with one quadrant on each wafer left un-implanted. **Fig. 1a** outlines the post-implantation process, all implanted samples were annealed at 1700 °C for 30 minutes in an argon ambient, where the surface was protected by a carbon capping layer formed by the pyrolysis of photo-resist. This layer was subsequently removed through O_2 plasma ashing, followed by a sacrificial thermal oxidation at 1050 °C for 20 minutes to ensure complete carbon removal. The wafers were then cleaned with RCA and HF rinse. For the DLTS / MCTS measurements, Schottky diodes were fabricated by depositing a 100 nm nickel layer on the Si-face of the diced chips from each quadrant, with a semi-transparent contacts for MCTS measurements with optical excitation and a thicker central contact for DLTS measurements. The contact diameter for implanted wafer were 1 mm and for pristine (reference) sample was 1.5 mm.

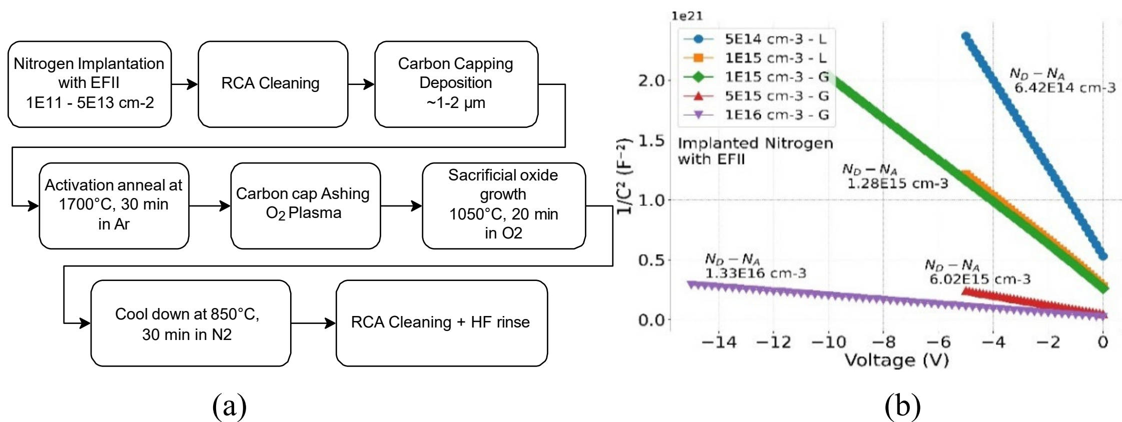

Fig. 1. Figure (a) illustrates post implant annealing steps for activation of dopants, and Figure (b) illustrates the calculated net-carrier density from the $1/C^2$ vs V plot measured for each sample to verify the implanted concentrations.

The measurement parameters were chosen to optimize the defect characterization and analysis of each sample. For the DLTS measurements, the period width, T_w, ranged from 19.2 ms to 1.92 s, with an electrical pulse stepping from a reverse bias of U_R = −1.5 to −10 V up to a pulse voltage of U_P = 0 V, with a pulse duration of t_p = 1 ms. In the case of MCTS measurements, the 365nm LED

was pulsed for 300 ms while maintaining a reverse bias at $U_R = -1.5$ V to -10 V, respectively for each sample. In order to capture the entire transient, the period width used ranged from 19.2 ms to 1.92 s.

Results and Discussions

Fig. 1b shows the plots of $1/C^2$ vs V of all implanted samples ranging from concentrations 5E14 cm^{-3}- 1E16 cm^{-3}. The highly linear nature of each plot shows the uniform doping concentration over depth, which is the intrinsic property of EFII implantation. The lowest implanted concentration 1E14 cm^{-3} and no implant regions were measured but the capacitance values were unrealistic due to very low doping levels. This linear slopes verifies the implanted Nitrogen concentrations to the net carrier density expected after activation annealing of the samples. The negligible variation of obtained net carrier concentration $N_D - N_A$ value compared to the implanted Nitrogen concentration is due to the existing background doping and tolerances in dose measurement systems for each sample.

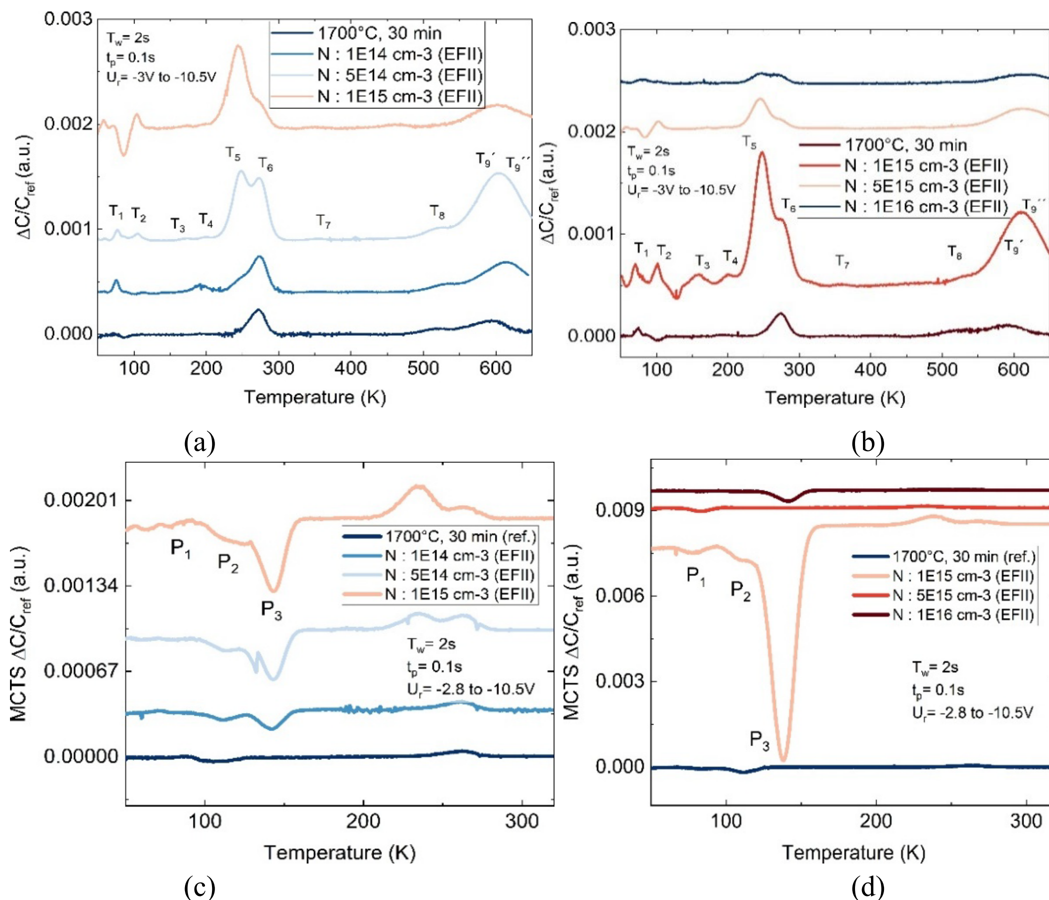

Fig. 2. DLTS peak progression in (a) and (b) shows the influence of EFII implanted Nitrogen concentration, while MCTS peaks for wafers L and G are shown in (c) and (d), respectively.

Deep level Transient Spectroscopy.

Analysis of the DLTS spectra revealed a total of ten dis-tinct deep-level defect peaks labeled in Fig. 2a and 2b corresponding to implanted wafers L and G respectively. Their corresponding energy levels and densities detailed in the Table 1. The data for the un-implanted (1700 °C, 30 min) sample serves as an important baseline for measurements specific to each wafer used. This sample shows minimal defect signals, especially compared to the implanted samples. This highlights that the high-temperature annealing effectively mitigates or eliminates native defects or those introduced during wafer processing. The prominent peaks in the implanted samples are therefore a direct consequence of the nitrogen implantation, and not the annealing process itself.

The dominant peaks, designated as T_6, has an activation energy of (E_c−0.681 eV) with a density of 6.28E12 cm^{-3}, and is assigned to either ON0b or the well-known $Z_{1/2}$ defect. A closely related peak, T_5, was observed at (E_c−0.586 eV) with a density of 1.06E13 cm^{-3}, and is assigned to the ON0a which is a carbon complex found in samples that were subjected to carbon injection experiments [5,6]. Hence ON0a is suggested to be stable defect with di-interstitial carbon.

Table 1. The list of peaks observed in the Deep Level Transient Spectroscopy (DLTS) measurements between 50-650 K temperature range.

Peaks	Energy (eV)	Energy SD (eV)	σ ($\times 10^{-15}$ cm^{-2})	N_t ($\times 10^{13}$	Assignment cm^{-3})
T_1	E_c - 0.133	0.009	0.151	0.207	SD1 / Ti [2, 7]
T_2	E_c - 0.213	0.015	0.899	0.186	$E_{0.22}$ [8]
T_3	E_c - 0.39	0.02	2.34	0.127	$E_{0.38}$ [6, 9]
T_4	E_c - 0.40	0.088	0.205	0.164	S1 / EH1 [10, 11]
T_5	E_c - 0.586	0.129	3.32	1.061	ON0a [6]
T_6	E_c - 0.681	0.042	6.36	0.628	ON0b / Z1/2 [2, 3, 6, 10, 11]
T_7	E_c - 0.729	0	0.083	0.0393	EH3 / S2 [11–13]
T_8	E_c - 1.183	0.156	6.59	0.167	EH4/5 [14] / ON2b [2, 13, 15]
T_9’	E_c - 1.391	0.066	4.10	0.368	SD2 [16] / EH6 [7, 12, 13]
T_9”	E_c - 1.532	0.112	9.9	0.764	EH6/7 [2, 3, 7, 8, 13, 16]

In addition to these prominent carbon-related complexes, peak T_4 associated with activation energy (E_c−0.40 eV), assigned to S_1/EH_1 which could be V_{Si} due to implantation process involved, due to their overlapping nature, accurate assignment is not possible. and T_7 at (E_c−0.729 eV), assigned to S_2 related to (C_i)(V_{Si}). Other defects detected include T_1 at (E_c−0.133 eV) related to Titanium, T_2 at (E_c−0.22 eV) cited in [8] are material or vendor specific defects and T_3 at (E_c−0.39 eV), the previously observed ($E_{0.38}$) is the metastable defect related to mono C_i . The deepest traps are T_8 at (E_c−1.183 eV) are assigned to ($EH_{4/5}$) relating to the carbon anti-site vacancy (CAV) pair or ON2b, T_9′ at (E_c−1.391 eV) assigned to (SD_2/EH_6) which could be a [Titanium - Nitrogen] interaction trap as mentioned in [16] and the well-documented $EH_{6/7}$ defect (T_9′′) at (E_c−1.532 eV) with a density of 7.64E12 cm^{-3} was measured. The carbon interstitial complexes observed in this study are expected to be formed due to the Nitrogen implantation process where the Carbon is kicked out from its site creating a vacancy which is then occupied by nitrogen at 1700 °C activation anneal. This is proved by the net carrier density value measured which is close to the implanted nitrogen concentrations.

Minority Carrier Transient Spectroscopy

A light pulse duration of 300 ms for hole trap filling was selected based on preliminary observations of the capacitance transients. This duration was empirically determined to ensure the charging process reached a steady state. Consequently, the combination of light intensity and pulse length employed in this experimental setup justifies the assumption of complete trap saturation within the probed volume. Furthermore, the use of semi-transparent contacts ensures that the photo-excited volume aligns closely with the volume electrically interrogated under reverse bias. Given these considerations, the calculated trap density provides a fair estimate of trap density for hole carriers. Beyond absolute quantification, this methodology facilitates a relative comparison across the samples, which remains a primary focus of this investigation. The MCTS measurements reveal three distinct peaks for the minority (hole) carriers as shown in Fig. 2c and 2d and listed in Table 2. Each peaks are labeled as, P_1, P_2 and P_3. Peak P_1 at (E_V+0.171 eV) which can be assigned to X relating to Al in the material was observed on all the samples, peak P_2 at (E_V+0.259 eV) assigned to the B′ defect, which is the shallow B-center on the shoulder of Peak P_3, and the dominant peak P_3 at E_V+0.294 eV assigned to the B″ defect is the deeper B-center which were resolved in both

experimental and theoretical studies [11, 15, 17]. Both boron peaks that overlap at 125K - B′ and B″ were separated based on hexagonal or pseudo cubic location of Boron in Silicon site. Influence of B" on Nitrogen implant concentration is witnessed in this study. An additional peak, P_4, was observed in the pristine sample at (E_V+0.881 eV) and (E_V+0.893 eV).

Table 2. The list of peaks observed in the Minority Carrier Transient Spectroscopy (MCTS) measure-ments between 50-650 K temperature range.

Peaks	Energy (eV)	Energy SD (eV)	σ ($\times 10^{-15}$ cm^{-2})	N_t ($\times 10^{13}$ cm^{-3})	Assignment
P_1	$E_V + 0.171$	0.0211	1.226	0.154	X [15]
P_2	$E_V + 0.259$	0	6.370	0.133	B′ [11, 15, 17]
P_3	$E_V + 0.294$	0.0217	0.345	2.51	B″ [11, 15, 17]
P_4	$E_V + 0.881$, $E_V + 0.893$	–	–	–	Found on Pristine Wafer only

Further, the pristine as-grown 4H-SiC epitaxial layer with background doping of 5E15 cm^{-3} was subjected to identical DLTS and MCTS measurements. The deep level spectrum between 50-650 K are compared with the highest dose of Nitrogen implant with EFII of 1E16 cm^{-3} from another wafer. In Fig. 3a, it is evidently visible that the only difference in defect landscape being the Carbon complex (ON0a) peak at 250 K and the $EH_{4/5}$, $EH_{6/7}$ at 520 K and 600 K respectively. The other shallow peaks between 50-200 K are material/vendor specific defects traps. The magnitude of DLTS signal indicates that the EFII process is not creating significant trap concentration at 1E16 cm^{-3} Nitrogen concentrations and the signal value is in the same range of an operational SiC power devices. Sim-ilarly, in Fig. 3b, The MCTS signal show dominant peak of Deep Boron center (B") which is not a nitrogen related minority carrier trap. Notably, there are no other hole traps(D center) generated with nitrogen implantation using EFII process on all the EFII implanted samples. This indicates that the EFII process do not generate the lifetime killer D-center. The detected B centers could be due to the vendor specific Boron from reactors used for CVD growth. Overall, the estimated trap densities for the dominant peaks on implanted samples related to ON0a and carbon vacancy peak $Z_{1/2}$ for pristine sample using the equation 1 [15] is 3.4E12 cm^{-3} and 1.8E12 cm^{-3} respectively. This indicates that the trap densities are in the standard operational range for power devices in 4H-SiC material.

$$N_T = 2 \cdot N_D \cdot (\Delta C / C_{ref}) \qquad \text{when } N_T \ll N_D \tag{1}$$

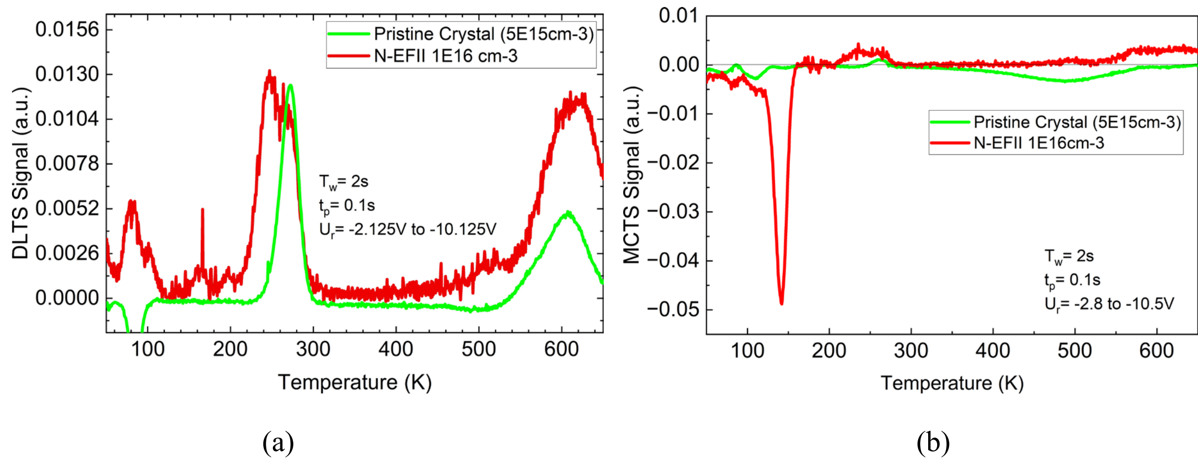

(a) (b)

Fig. 3. (a) Comparision of DLTS peaks observed in the pristine crystal and the 1E16 cm^{-3} EFII implanted Nitrogen. Similarly, (b) Comparision of MCTS peaks from same samples. Note: Wafers are from different vendors.

Summary

In this work we have detected and assigned the trap levels introduced in 4H-SiC epitaxial grown material by performing Nitrogen implantation with Energy Filtered Ion Implantation technology, based on matching the defects activation energy and capture cross-section from earlier work, it is shown that there are no new defect signatures that were detected between 50-650 K in either DLTS or MCTS measurements. ON0a and $EH_{6/7}$ are the dominant electron traps detected in the DLTS spectra and Shallow B centers are the dominant hole traps detected in MCTS spectra. No D-center was found on any EFII implanted samples. The estimated trap densities of these defects are in the typical trap density range for SiC power device operation. However, further study on separating the overlapping signal peaks between the temperature range 200-300K and 500-650K can be performed to clearly understand the defect structure and create a foundation for further trap studies in ion implanted 4H-SiC samples.

Acknowledgement

All Ion implantations were done at Ion Beam Center (IBC), Helmholtz-Zentrum Dresden-Rossendorfe.V. (HZDR) Dresden, Germany. The Activation anneal was performed at Fraunhofer Institut für In-tegrierte Systeme und Bauelemente technologie (IISB), Erlangen, Germany.

References

[1] Tsunenobu Kimoto. Fundamentals of Silicon Carbide Technology. *Wiley-IEEE Press*, (1st), November 2014.

[2] J. Erlekampf, M. Rommel, K. Rosshirt-Lilla, B. Kallinger, P. Berwian, J. Friedrich, and T. Erlbacher. Lifetime limiting defects in 4H-SiC epitaxial layers: The influence of substrate originated defects. *Journal of Crystal Growth*, 560–561:126033, April 2021.

[3] Koutarou Kawahara, Giovanni Alfieri, and Tsunenobu Kimoto. Detection and depth analyses of deep levels generated by ion implantation in n- and p-type 4H-SiC. *Journal of Applied Physics*, 106(1):013719, July 2009.

[4] Constantin Csato, Florian Krippendorf, Shavkat Akhmadaliev, Johannes Von Borany, Weiqi Han, Thomas Siefke, Andre Zowalla, and Michael Rüb. Energy filter for tailoring depth profiles in semiconductor doping application. *Nuclear Instruments and Methods in Physics Research Sec-tion B: Beam Interactions with Materials and Atoms*, 365:182–186, December 2015.

[5] Marianne Etzelmüller Bathen, Margareta Linnarsson, Misagh Ghezellou, Jawad Ul Hassan, and Lasse Vines. Influence of Carbon Cap on Self-Diffusion in Silicon Carbide. *Crystals*, 10(9):752, August 2020.

[6] Marianne Etzelmüller Bathen, Robert Karsthof, Augustinas Galeckas, Piyush Kumar, Andrej Yu. Kuznetsov, Ulrike Grossner, and Lasse Vines. Impact of carbon injection in 4H-SiC on de-fect formation and minority carrier lifetime. *Materials Science in Semiconductor Processing*, 176:108316, June 2024.

[7] Franziska C. Beyer. *Deep Levels in SiC*. Department of Physics, Chemistry and Biology, Linköping University, Linköping, 2011.

[8] O. V. Feklisova, E. E. Yakimov, and E. B. Yakimov. Study of single-layer stacking faults in 4H–SiC by deep level transient spectroscopy. *Applied Physics Letters*, 116(17), April 2020.

[9] Robert Karsthof, Marianne Etzelmüller Bathen, Augustinas Galeckas, and Lasse Vines. Conver-sion pathways of primary defects by annealing in proton-irradiated n -type 4 H -SiC. *Physical Review B*, 102(18):184111, November 2020.

[10] M. E. Bathen, A. Galeckas, J. Müting, H. M. Ayedh, U. Grossner, J. Coutinho, Y. K. Frodason, and L. Vines. Electrical charge state identification and control for the silicon vacancy in 4H-SiC. *npj Quantum Information*, 5(1):111, December 2019.

[11] Tihomir Knežević, Tomislav Brodar, Vladimir Radulović, Luka Snoj, Takahiro Makino, and Ivana Capan. Distinguishing the EH1 and S1 defects in n-type 4H-SiC by Laplace DLTS. *Ap-plied Physics Express*, 15(10):101002, September 2022.

[12] J. Erlekampf, B. Kallinger, J. Weiße, M. Rommel, P. Berwian, J. Friedrich, and T. Erlbacher. Deeper insight into lifetime-engineering in 4H-SiC by ion implantation. *Journal of Applied Physics*, 126(4):045701, July 2019.

[13] Takafumi Okuda, Giovanni Alfieri, Tsunenobu Kimoto, and Jun Suda. Oxidation-induced ma-jority and minority carrier traps in n- and p-type 4H-SiC. *Applied Physics Express*, 8(11):111301, October 2015.

[14] Marianne Etzelmüller Bathen, Robert Karsthof, Ulrike Grossner, and Lasse Vines. Stabil-ity, Evolution and Diffusion of Intrinsic Point Defects in 4H-SiC. *Materials Science Forum*, 1062:371–375, 2022.

[15] Marianne Etzelmüller Bathen, Piyush Kumar, Misagh Ghezellou, Manuel Belanche, Lasse Vines, Jawad Ul-Hassan, and Ulrike Grossner. Dual configuration of shallow acceptor levels in 4H-SiC. *Materials Science in Semiconductor Processing*, 177:108360, July 2024.

[16] A. A. Lebedev. Deep level centers in silicon carbide: A review. *Semiconductors*, 33(2):107–130, February 1999.

[17] Vitor J. B. Torres, Capan Ivana, and José Coutinho. Theory of shallow and deep boron defects in 4H-SiC. *Physical Review B*, 106(22), 2022.